ScienSage

Journal of Advanced Scientific Research

Available online through http://www.sciensage.info

ISSN
0976-9595
Research Article

EFFECTIVE SOLOCHROME DYE DEGRADATION USING SYNTHESIZED COPPER DOPED TITANIUM DIOXIDE NANOPARTICLES

A M Kalamma[1], T Subba Rao[1], Ambreen Saba Mulla[2], Mohammed Afzal*[2], Shirajahammad M.Hunagund[3]

[1]*Department of Physics, Shri Krishnadevaraya University Ananthapuramu, Andhra Pradesh, India*

[2]*Department of Physics, SECAB's A.R.S.I Degree College for Women, Vijayapur, Karnataka, India*

[3]*Department of Physics, SECAB's I.E.T College, Vijayapur, Karnataka, India*

**Corresponding author: mdafzal12@gmail.com*

ABSTRACT

A simple hydrothermal route was used for the synthesis of pristine and Cu-doped TiO_2 nanoparticles (NPs) using EDTA (di-sodium salt dehydrate) as the capping and reducing agent. In order to study the optical, functional, surface morphology, structure and elemental analysis of synthesized nanoparticles were subjected to UV-Vis spectrophotometer, FESEM, XRD and EDS. From these results UV-Vis characterization reveals that synthesized particles are having absorption maxima is around 341 and 250.23 nm and using Tauc's plot the estimated E_g values were found to be 3.07eV and 2.84 eV respectively. FESEM of particles reveal that they are having the spherical cluster with average size of about 10 nm to 20 nm. EDS spectrum confirms the presence of elements Ti and O. From the XRD pattern it confirms that they are having anatase phase, tetragonal and cubic crystal structure for TiO_2 and Cu-TiO_2 respectively . Further, the photocatalytic degradation of solochrome dye was performed under UV irradiation using these synthesized nanoparticles. Interestingly, it was observed that the relative absorption intensity continuously decreased as the UV illumination exposure time increased, significantly indicating that solochrome dye degraded effectively on the surface of bare and Cu doped TiO_2 photocatalyst.

Keywords: Copper doped titanium dioxide, Hydrothermal, Dye degradation.

1. INTRODUCTION

Organic dyes is one of the major groups of pollutants widely used in textile, plastic, medicine and many other industries, while the hazardous effects of organic dyes in waste water have been a major concern and now a major threat in the environment due to the substantial pollution problems caused by them. These industries exhausted large quantity of high content color effluents, which are generally more toxic and resistant to destruction by conventional methods. A necessary criterion in the use of these dyes is that they must be highly accumulated in water and stable in light during washing. The accumulation of these dyes in the water bodies causes eutrophication, reduces the reoxygenation capacity and makes severe damage to the aquatic organisms by hindering the infiltration of sunlight [1]. They must also be resistant to microbial attack. Therefore, they are not readily degradable and are typically not removed from water by wastewater treatment systems and conventional methods like adsorption, ultra filtration, chemical and electrochemical methods [2]. The superiority of photocatalytic degradation by nanoparticles in wastewater treatment is due to its advantages over the conventional methods, such as quick oxidation, no formation of polycyclic products and oxidation of pollutants. It is an effective and rapid technique in the removal of pollutants from wastewater [3]. In the recent years, numerous metal oxides including TiO_2 [4], ZnO [5], and other oxides have attracted growing attentions for photodegradation of organic dyes; TiO_2 is of particular interests due to its low cost and high stability. Nonetheless, TiO_2 has been gained remarkable attention as a photocatalyst in degradation of organic pollutants. Due to the properties of anti- oxidation long term stability, non-toxicity, strong redox ability, it has been widely used in the field of photocatality. TiO_2 being a semi conductor with a large band gap *i.e,* 3.2, 3.02 and 2.96 eV for anatase, rutile and brookite phases respectively. As TiO_2 particles, get irradiated by photons with energy greater than the band width of TiO_2, the valence band electrons will be transited to the

band of conduction which leave holes in the valence band. Now electron hole pairs could participate into all kinds of chemical reactions on TiO_2 surface and that ultimately degrades all the pollutants in the solution. This reaction leads to recombination of electrons and holes quickly; eventually TiO_2's photocatalytic activity greatly decreases. To obtain higher photocatalytic activity, one commonly used method is doping metal and /or non metal ions into the TiO_2's crystal lattice. Sahoo and Gupta [6-10] synthesized Ag and Fe ions doping micro crystalline TiO_2 followed by a liquid impregnation technology. They found that Ag doped with TiO_2 could be degraded up to 99% of the pollutants under the UV light. For the visible light Fe doped with TiO_2 could be degraded more than 96% and 90% for methylene blue and methyl blue respectively. Vu *et al.* [11-15] synthesizing highly active photocatalytic TiO_2 nano tubes by hydrothermal treatment in the base medium using the commercial powder of TiO_2 as Ti source. The non-metal doped with TiO_2 samples were made using urea, ammonium fluoride, thioura and ethylene glycol by post synthesis as N, S, F and C source. Degradation of Rhodamine B indicated, a non metal being doped TiO_2 samples, exhibited very high photocatalytic activity under visible light compare to that with non doped TiO_2 samples. Choi *et al* [16-19] successfully prepared TiO_2 nanoparticles doped with 21 different metal ions by sol-gel method and found that metal ions significantly influenced the photo reactivity, charge carrier recombination and interfacial electron transfer rates. Anatase phase is active for photocatalytic phenomena based on the chemical and dynamic properties of organic compounds degradation. Observing all the potential of TiO_2, here in, we have synthesized TiO_2 and Cu doped TiO_2 nano particles and analysed their photocatalytic solochrome dye degradation under the UV light.

2. MATERIAL AND METHODS

2.1. Chemicals

Titanium (IV) n butoxide (TNB) wt 99% liquid analytical grade, Copper nitrate hexahydrate [$Cu(NO_3)_2$.$6H_2O$] and EDTA (di-sodium salt dehydrate) were purchased from Alfa Aesar Chemicals, India. De-ionized water (DW) was used in the preparation of all solutions.

2.2. Synthesis of $TiO_2$and Cu doped nanoparticles

Titanium dioxide Nano particles were synthesized via hydrothermal route [20]. Here 30ml of 0.1M of E. D. T.A ($C_{10}H_{14}N_2Na_2O_8.2H_2O$) was prepared by dispersing 0.56gm in 15ml of de-ionised water (DW) with a continuous stirring with the aid of magnetic stirrer for 10 minutes, later added 15ml of DW and 5ml of 0 .1M $Cu(NO_3)_2$. $6H_2O$, then 1ml of Titanium (IV) n-butoxide was added drop wise with continuous stirring for 30 minutes. The colloidal solution was then transferred to a 50ml Teflon-lined stainless steel auto clave, the autoclave was sealed and placed in an oven heated up to 180°C for 3hours, then the autoclave was cooled down to room temperature. Under ambient conditions, the reactant mixture was centrifuged to collect the product; the product was washed continuously with DW several times to remove the organic molecules bonded to the surface of the product. The final product was dried in an oven at100 °C for one hour and the same procedure, as adopted in Cu-TiO_2 (CTO NPs) was used to synthesize TiO_2 (TO NPs) without adding dopant and the sample was then used for Photodegradation application.

2.3. Photocatalytic experiments

The photocatalytic reactor is a Pyrex-glass cell with 1.0 L capacity. A 10 W Lamp (Philips) as the light source (365 nm) was placed in a quartz lamp holder which immersed in the photo reactor cell. Before illumination, the solution was allowed to stir in dark for 60 minutes to achieve adsorption-desorption equilibrium between the dye and photocatalyst. The cell was filled with 1mg/L of dye solution and 1 x 10^{-5} M of the photocatalyst. Magnetic stirrer was used to introduce fresh air bubbles into the suspension using a pump. Dye degradation was examined by taking 4 mL of the suspension at 10 minutes irradiation time intervals. Finally, the rate of degradation was determined from the change in absorbance of Dye solution. Before the measurement, the solution was centrifuged for 10min at 5000 rpm to remove any turbidity. All kinetic data were evaluated using Microsoft Excel 2010 program.

2.4. Characterization techniques

2.4.1. UV-Vis spectroscopy

UV-Vis absorbance spectra in the wavelength range 200-800nm was measured using UV-Vis spectrophotometer (model: SPECORD 200+ Analytik-jena).

2.4.2. XRD

The crystal structure of the powder sample at a scanning rate of 0.02^0 per second in the range of 20^0 to $80^0$with the use of Cu K_α radiation of wavelength 1.54060Å were analysed by XRD (model: Rigaku pro analytical) at MIT Manipal. Peak analysis was carried out using PCPDFWIN software.

The surface morphology and nano nature of the samples at an operating voltage 5kV were examined using FESEM (model: xford-EDX system IE 250 X Max 80) At Mangalore university, Mangalore.

2.4.3. EDS

Elemental compositions were analysed using EDS (model:FEI Quanta 200 F) At Mangalore university, Mangalore.

2.4.4. Zeta potential

The zeta potential was based on the surface charge of the particles relative to the local environment of the prepared particle. This electrostatic potential of shear plane of the particle was carried out in ultrasonicated dispersion of 0.01 g/100 mL in DMSO at room temperature using the Horiba SZ-100 nanoparticle analyzer.

3. RESULTS AND DISCUSSION

3.1. Optical properties

3.1.1. UV-Vis Spectroscopy

UV-Vis Spectra were recorded for TO NPs and CTO NPs in an ethanol solvent at room temperature and are shown in Fig 1(a) and (b).

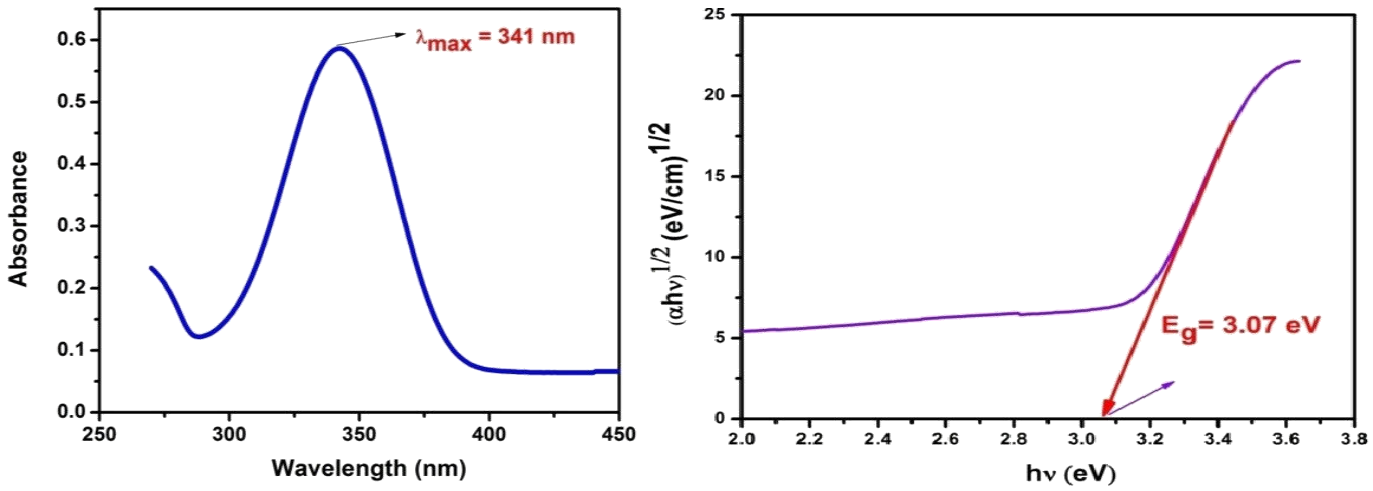

Fig. 1a: UV and Tauc's plot TiO_2

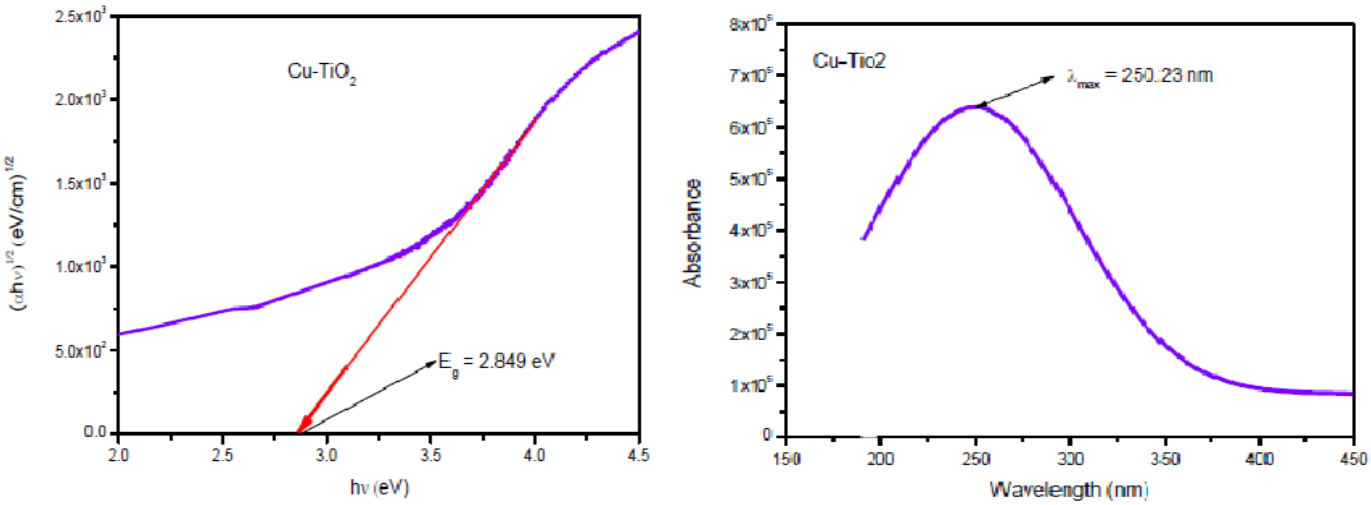

Fig. 1(b): UV and Tauc's plot Cu- TiO_2

From the Fig.1 (a) and (b), it is observed that the absorption maxima (λ_{max}) for TO NPs and CTO NPs were found to be 341 nm and 250.23 nm respectively which is a preliminary indication for the presence of TiO_2 material. The band gap of both the samples were estimated using the absorption data with the help of (K-M) transformation method [21].Band gap energy of the semiconductor was estimated using the optical absorption coefficient (α) and is expressed by equation

$$\alpha = \frac{A(h\nu - E_g)^{1/n}}{h\nu} \quad (1)$$

Where, hν is an energy of photon, E_g is the band gap energy, A is a constant depends on the transition probability and depends on the nature of the transition for allowed direct transition n= ½, for allowed indirect transition n=2. In our cases for an indirect gap, the value of n is 2 for TO NPs and CTO NPs. Using Tauc's plot the estimated E_g values were found to be 3.07eV and 2.84 eV respectively.

3.2. Structural properties

XRD analysis was carried out to verify the presence of nano crystalline and phase formation.

Fig 3 (a and b) shows XRD patterns for TO and CTO powders respectively it is observed that the presence of strong and sharp peaks; it may indicate the formation of the well crystallized samples. From the Fig 3 (a) it is observed that the Bragg's reflection at 2Θ= 25.3429, 37.8769, 47.9727, 54.0791, 62.7467, 75.1348 and 82.6813 can be indexed to (101), (004), (200), (211), (204), (215) and (224) crystal planes respectively. The comparison of 2Θvalues in observed Fig 3(a) XRD patterns with those from the standard Joint Committee on Powder Diffraction Standards (JCPDS) data no. 89.4921 confirms the formation of the TiO_2 phases having anatase phase and tetragonal crystal structure. Fig 3(b) shows the XRD patterns for CTO powders, it is observed that the Bragg's reflection at 2Θ= 25.3803, 37.8187, 47.9622, 54.1718, 62.7795, 68.9548, 75.0959 and 82.8946 can be indexed to (311), (422), (442), (444), (731), (822), (753) and (844) crystal planes respectively. The comparison of 2Θ values in observed Fig. 3(b) XRD patterns with those from the standard Joint Committee On Powder Diffraction Standards (JCPDS) data no. 81.1611 confirms the formation of the Cu-TiO_2 having Anatase phase and Cubic crystal structure. The Scherer's equation [22] is used to estimate an average crystalline size by determining the full width at half maximum (FWHM) of the most intense reflection plane and this equation is given by

$$D \approx \frac{0.9\lambda}{\beta \cos\theta} \quad (2)$$

Where D is an average crystalline size, λ is the wavelength of X-ray used (1.50406 x 10^{-10} m), Θ is the Bragg's angle in radian and β is the full width at half maximum of the most intense reflection in radian. In our case, the most intense peak for TO and CTO were found to be (101) and (311) plane and the estimated average crystalline size is 7.362 nm and 6.098nm respectively.

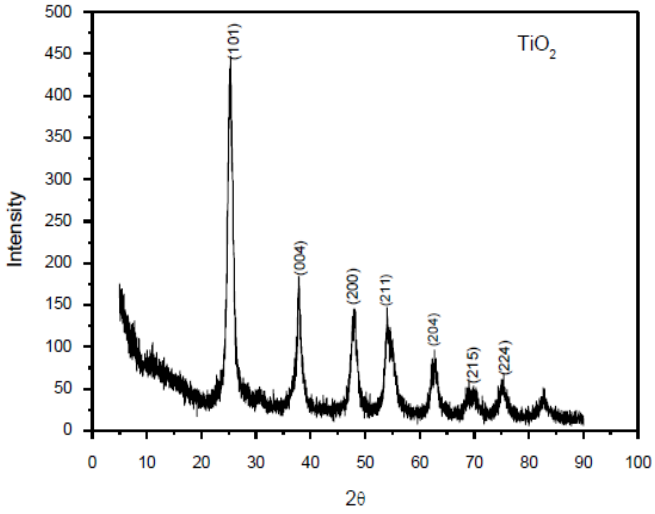

Fig. 3 (a): XRD graph for TiO_2

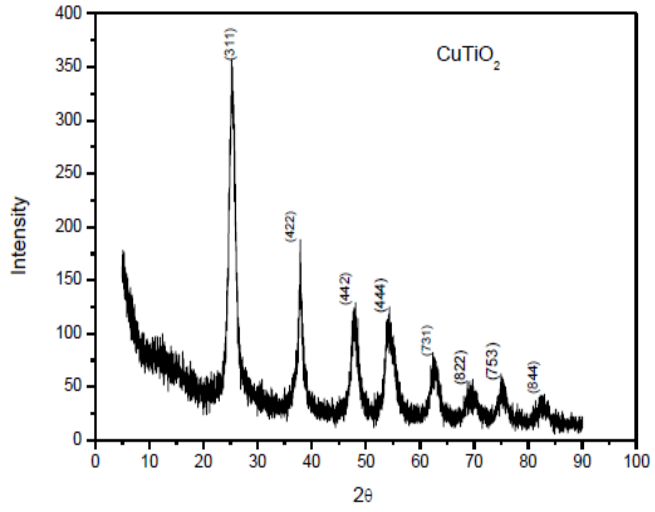

Fig. 3 (b): XRD graph for Cu-TiO_2

3.3. Morphology, Size Distribution and Elemental Analysis

FE-SEM analysis was used to examine the surface morphology and nano nature of the samples. Fig 4 (a and b) shows the particles are having the spherical cluster with average size of about 10 nm to 20 nm. EDS was examined to investigate the chemical composition in CTO NPs. Fig 4 (c and d) represents the EDS spectrum for TO NPs and CTO NPs, hence EDS spectrum confirms the presence of elements i.e. Ti and O, in addition small quantities of element C was observed since it is residue of oil contaminants. The weight percentage (%) and atomic weight percentage (%) CTO NPs are shown in Fig 4 (c and d).

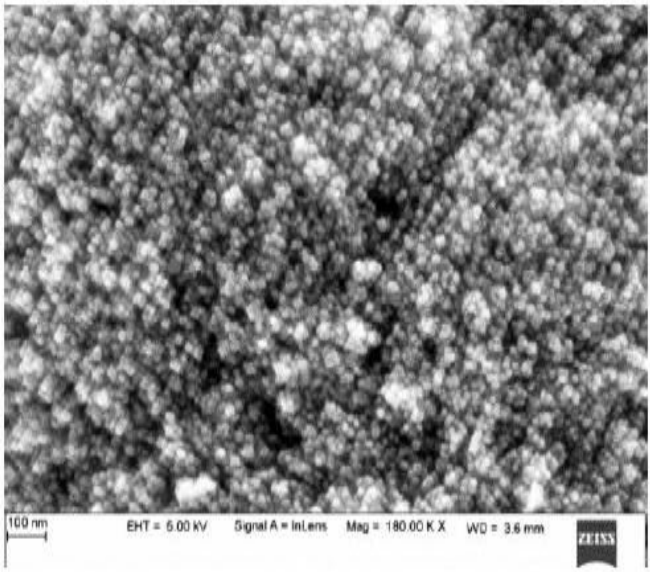

Fig. 4(a): FE- SEM image of TiO_2

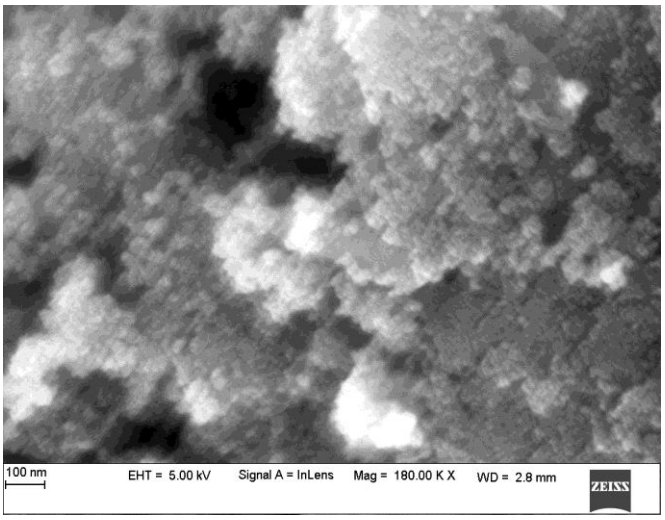

Fig. 4(b): FE- SEM image of Cu-TiO_2

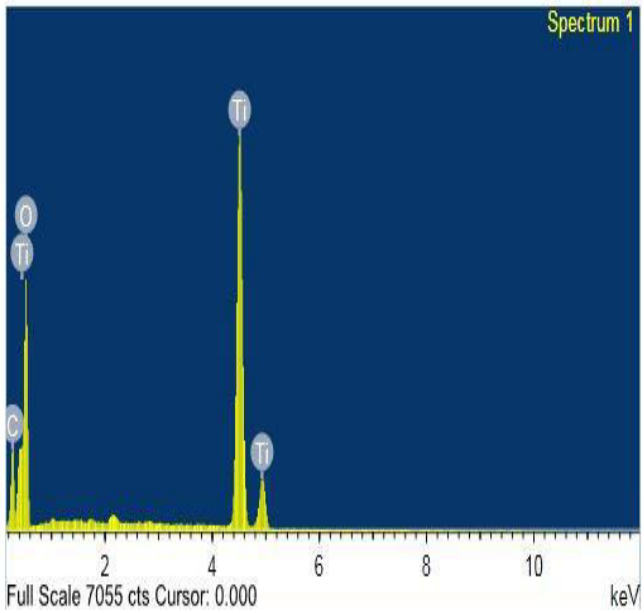

Fig. 4(c): EDS spectrum of TiO_2 NPs corresponding weight % and atomic % of element O - 61.19, 55.18 ; Ti - 57.22,17.23 and C - 22.97,27.59 respectively.

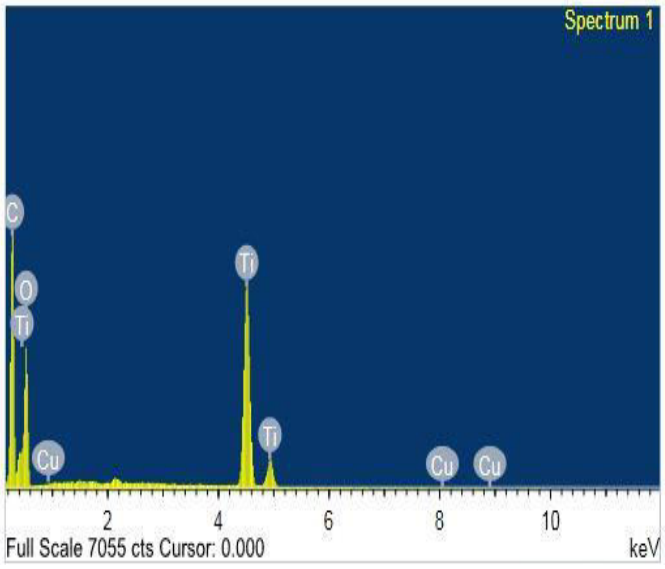

Fig. 4(d): EDS spectrum of Cu-TiO_2 NPs corresponding weight % and atomic % of elements O -36.48,55.71; Ti - 32.27,19.46 and C - -0.06,-0.02 respectively.

3.4. Zeta Potential Study

The zeta potential with a positive value of 30 mV with electrophoretic mobility 0.000061 cm^2/Vs and with positive value of 22.9 mV with electrophoretic mobility 0.000047 cm^2/Vs suspension was obtained

for the TO and CTO NPs respectively in DMSO and the zeta potential graphs shown in the **Fig. 5**, which clearly indicates a stable dispersion without particle settlement. Furthermore, the study of prepared suspension corroborates with general criteria of zeta potential (ξ) value 30 mV with positive or negative sign for better stability.

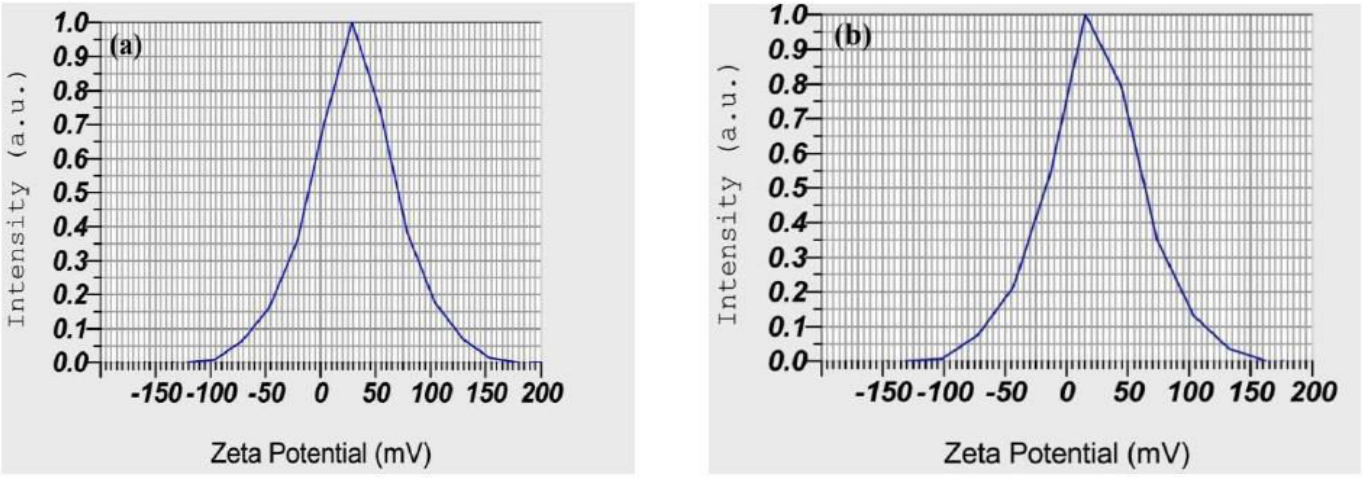

Fig. 5: Zeta potential evaluation of (a) TO NPs and (b) CTO NPs in DMSO solvent.

3.5. Photodegradartion process

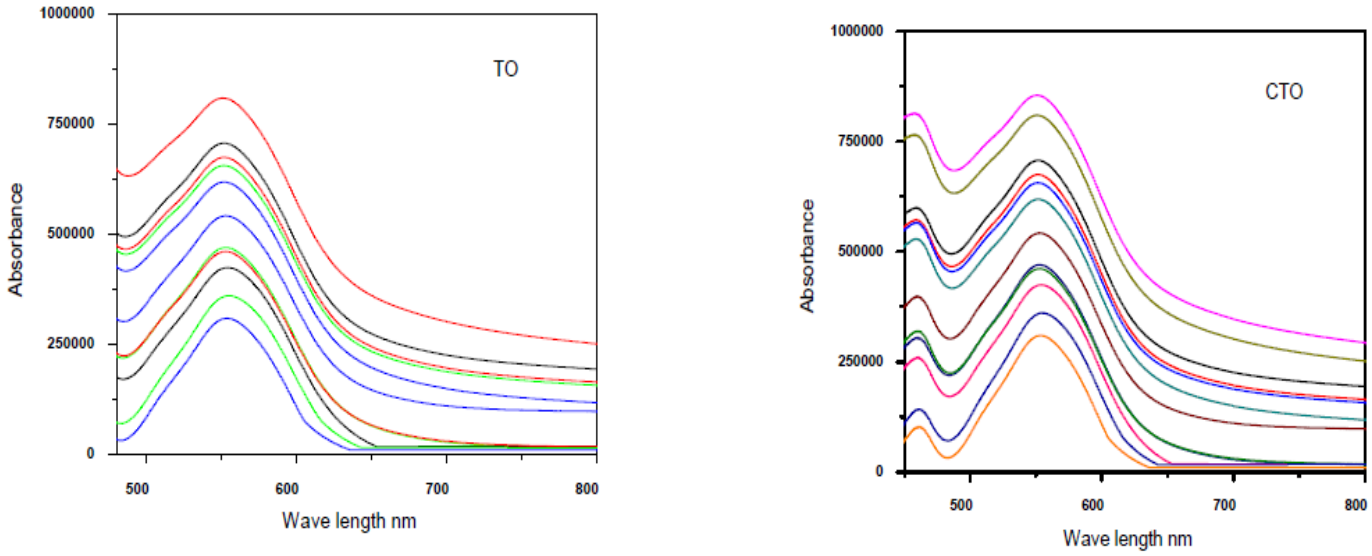

(a) **(b)**

Fig. 6: Photo degradation evaluation of (a) TO NPs and (b) CTO NPs in solo chrome dye solution

3.6. Evaluation of photocatalytic activity

To evaluate the photocatalytic activity of TO NPs, the photocatalytic degradation of solochrome dye was performed under UV irradiation. The photocatalytic degradation was evaluated by measuring the absorbance at regular time intervals. Interestingly, it was observed that the relative absorption intensity continuously decreased as the UV illumination exposure time increased, significantly indicating that solochrome dye degraded effectively on the surface of TO photocatalyst [Fig. 6 (a) & (b)]. This is because, under illumination, highly oxidizing hydroxyl and oxy radicals are formed by the semiconducting metal oxides like TO, CTO etc. via generation of electron-hole pairs, which break the large organic materials into less harmful small organic materials. The obtained degradation was 63 % and 76 %

within 120 min for TO and CTO respectively [23]. It reveals that after doping with Cu, percentage of degradation was increased.

4. CONCLUSION

Eco friendly hydrothermal route was used for the synthesis of TiO_2 (TO) and Cu doped TiO_2 (CTO) nanoparticles. It was confirmed by various characterization techniques that TO and CTO are having grain size about 10 to 20 nm. Further studies showed that, Solochrome dye was degrading under UV light using TiO_2 and Cu doped TiO_2 nanoparticles. Among doped TiO_2, the maximum degradation efficiency was found to be 63 % for TO and 76% for CTO. From this it is confirmed that CTO is more efficient catalyst for degradation of dye.

5. REFERENCES

1. Faisal M, Tariq MA, Muneer M. *Dyes Pigm,* 2007; **72**: 233-239.
2. Tang W Z, An H. *Chemosphere,* 1995; **31**:4157-4170.
3. Sobana N, Muruganadham M, Swaminathan M. *J Mol Catal*, 2006; **258**:124-132.
4. El-Kemary M, Abdel-Moneam Y, Madkour M, El-Mehasseb I. *J Lumin*, 2011; **131**:570-576.
5. Ullah R, Dutta J. *J Hazard Mater*, 2008; **156**:194-200.
6. Sahoo C, Gupta, AK. *Journal Of Environmental Science And Health,* 2015; **50**:659-668.
7. Khan M, Gul SR, Li J. *Materials Research Express,* 2015; **2**:066201.
8. Wu GH, Zheng SK, Lv X. *Chinese Journal Of Inorganic Chemistry*, 2013; **29:**9-14.
9. Zhu XH, Liu JM. *Applied Physics*, A 2014; **117**:831-839.
10. Hussain ST, Mazhar M, Siddiqa A. *The Open Catalysis Journal*, 2012; **5**:21-30.
11. Vu TA, Dao CD, Hoang TT. *International Journal Of Nanotechnology*, 2013; **10**:235-246.
12. Zheng SK, Wu GH, Liu L, et al. *Acta Physica Sinica*, 2013; **62**:043102.
13. Yan CY, Yi WT, Yuan HM, et al. *Environmental Progress & Sustainable Energy*, 2015; **33:**419-429.
14. Yi WT, Yan CY, Yan P. *Journal of Sol-Gel Science and Technology*, 2014; **69**:386-396.
15. Wang Z, Li FF, Yang C, *Advanced Materials Research*, 2011; **233-235**:589-595.
16. Choi W, Termin A, Hoffmann RM, et al. *J. Phys. Chem* , 1994; **98**:13669-13679.
17. Zhang WY, Wang SJ, Li JG, et al. *Materials Research Innovation*, 2013; **17**:3-6.
18. Li FF, Wang Z, Yang C, et al. *Journal of Molecular Catalysis (China)*, 2012; **26**:174-183.
19. Hamadanian M, Reisi Vanani A, Majedi A. et al. *Applied Surface Science*, 2010; **256**:1837-1844.
20. Hunagund SM, Desai R Vani. *RSC Adv.*, 2016; **6**:97438-97444.
21. Hunagund MS, Desai RV, Barretto Delicia A, Pujar SM, Kadadevarmath SJ, Vootla S, Sidarai HA. *Journal of Photochemistry and Photobiology A: Chemistry*, 2017; **346**:159-167.
22. Patil PB, Kondalkar VV, Pawar NB. *RSC Adv.*, 2014; **4**:47278-47286.
23. Bagwan RB, Shaikh I, Malladi RS, Harihar AL, Hunagund SM. *Journal of Rare Earths,* 2020; **38:**234-240.